A Structure and Spectroscopy study about [16]Cycloparaphenylene Chiral Molecule

Baozhu Yang
Changzhou University
Shuang Huang (shuanghuang_cczu@163.com)
Changzhou University

Research Article

Keywords: theoretical research, [16]Cycloparaphenylene, π-electron system, aromaticity, chiral,

Posted Date: May 16th, 2023

DOI: https://doi.org/10.21203/rs.3.rs-2918278/v1

Version of Record: A version of this preprint was published at Theoretical Chemistry Accounts on July 14th, 2023. See the published version at https://doi.org/10.1007/s00214-023-02999-6.

Abstract

An interesting chiral molecule with a double half-twisted π-electron system has been investigated with theoretical calculations. To investigate the geometry and electronic structure, the size of macrocyclic cavity, electrostatic potential (ESP) and density-of-states (DOS) were calculated. The multi-center bond order (MCBO) and AV1245 index were calculated to compare the aromaticity of phenylene groups. To investigate the spectroscopic properties, Raman, Raman Optical Activity (ROA), UV-Vis spectrum, fluorescence, CPL (circularly polarized luminescence) and ECD (electronic circular dichroism) spectra have been calculated and analyzed. The oscillator strengths, rotatory strengths and dissymmetry factor (g_{lum}) have been discussed.

1. Introduction

Chiral molecules just as human hands, they are architecturally symmetrical, but one being the mirror-image of the other. One of the two mirror images is defined as enantiomer, whereas racemate is a solid, liquid, gaseous, or in solution composite of equimolar quantities of two enantiomeric species. The chiral molecule can be distinguished from its mirror-image with stereochemical descriptors, such as *R* and *S*, L and D, *P* and *M*, Δ and Λ. Left-handed and right-handed chiral molecules can exhibit different properties in stereoselective synthesis, and may lead to a result opposite to the original expectations. A painful example is thalidomide story. Left-handed thalidomide is a powerful tranquilizer, while the right-handed enantiomer has been proved to disrupt fetal development and cause congenital malformations. Over the past few decades, molecular chirality and related concepts have had a growing impact on science, going beyond the boundaries of chemistry, and with crucial implications in life sciences, materials sciences, and several other fields[1–6].

For the object to be chiral it must not have any inverse symmetry elements such as reflection planes or a center of symmetry. A simple chiral structure is a molecule with a chiral center, such as asymmetric C atom and N atom. There are other complicated types of chirality in molecules such as proteins and DNA structures. Recently, a special chiral molecule with a double half-twisted π-electron system was reported[7]. The molecule was referred to as [16]CPPL, ([16]cycloparaphenylene lemniscate, Fig. 1), which is connected by 16 phenylenes and stabilized by a rigid 9,9’-bicarbazole moiety, the whole structure represents figure-eight shape. The unique geometry of [16]CPPL makes it exhibit special photophysical and photoelectronic properties[8–9]. In this paper, we try to provide an in-depth theoretical calculation about the geometry structure, electronic structure and spectroscopic properties. We hope this paper will give us a deeper understanding about this interesting chiral molecule.

2. Computational details

Density functional theory (DFT) [10–11] was employed to optimize the stabilized structures with Gaussian 09 software package[12]. The spectroscopic properties related to the absorptions and emissions in CH_2Cl_2 solution were calculated by time-dependent density functional theory (TDDFT) [13–

14] with Truhlar's continuum solvation model based on the quantum mechanical charge density (SMD) [15]. The long-range-corrected functional ωB97XD functional[16–17] were selected in all the calculations. The TZVP [18–19] basis set was adopted for C, H and N atoms.

3. Results and discussion

3.1 Molecular Structure and Aromaticity.

The (*P*)-enantiomer of 16[CPPL] (right-handed) was optimized and shown in Fig. 1. For gas separation and catalysis process, the size of macrocyclic cavity is crucial. Therefore, we first measured the dimensions of 16[CPPL] and the size of cavitiy in it with Multiwfn software[20]. The length, width and height of 16[CPPL] are 30.6Å, 11.8Å and 13.2Å, respectively. The radius of the largest sphere in the hole is 2.25 Å. For extended π-conjugation molecule, aromaticity is a frequent topic of discussion. We sorted the 16 phenylene groups and compared the aromaticity of these groups in Fig. 2. The multi-center bond order (MCBO)[21], which is also known as multi-center index (MCI), and AV1245 index are calculated with Multiwfn software[22]. Larger value of the index implies stronger resonance and delocalization effect, and thus conjugation effect is strong and aromaticity of the ring is larger. As shown in Fig. 2, the two indexes basically follow the same trend that the central 9,9’-bicarbazole moiety with the number 1,8,9,16 phenylene groups have the smaller MCBO and AV1245 indexes. That means the conjugation effect of the central phenylene groups are weaker than that of two sides.

3.2 Electrostatic potential (ESP) and density of states (DOS)

The charge distribution on molecular surface has important effect on gas separation and catalysis, so we calculated the electrostatic potential (ESP) with Multiwfn software and shown them in Fig. 3. ESP measures the electrostatic interaction between a unit point charge placed at somewhere and the system of interest. A positive (negative) value implies that current position is dominated by nuclear (electronic) charges. Molecular ESP has been widely used for prediction of nucleophilic, electrophilic sites and the intermolecular interaction for a long time[23]. In Fig. 3, the negative values (nucleophilic sites) are localized on the surface of phenylene groups along the twisted lemniscate, while the positive values (electrophilic sites) appear on the side of phenylene groups.

To give an in-depth understanding about electron structure, density-of-states (DOS) and frontier molecular orbitals were shown in Fig. 4 and Fig. 5. For isolated molecule, the energy levels of molecular orbital are discrete, which are represented by vertical lines on the x-axis in Fig. 4, so we need to broad them with normalized Gaussian function. The black curve represents total-density-of-states (TDOS), while the red curve and blue curve correspond to the partial-density-of-states (PDOS) of central 9,9’-bicarbazole moiety and bilateral phenylenes, respectively. Overall, all the PDOS have the same trend, the bilateral phenylenes take a large percentage of molecular orbitals. The result looks reasonable since the number of bilateral phenylenes are more than central 9,9’-bicarbazole. It is obvious that the frontier MOs higher than − 0.30 a.u. mainly come from side phenylenes (blue curve), the HOMO-6 is composed by 9,9’-bicarbazole atomic

orbital, since there is a discrete red line. The details of frontier molecular orbitals are shown in Fig. 5, the HOMO is composed by π orbital of phenylene groups while the LUMO is composed by π* antibonding.

3.3 Raman, ROA, VCD and ECD spectra

On the basis of frequency calculations, Raman and Raman Optical Activity (ROA) in SCP(180) form were simulated and shown in Fig. 6. The Raman spectrum measures the intensity of scattered light and ROA spectrum measures the difference between scattering intensity of right and left circularly polarized light, respectively. From these two curves, there are obvious scattering responses near 1300nm -1400 nm and 1700 nm. We analyzed these vibration modes with Gaussview software [12] and these vibrations are caused by the bonds stretching in the plane of phenylene groups.

The important absorption data in CH_2Cl_2 solution were listed in Table 1. As we know, the single-electron excitation usually was represented as mixed transition of multiple MO pairs with corresponding weighting coefficients. It is hard to know where the electron is coming from and where it is going to. To explore the nature of single-electron excitation, hole-electron analysis proposed by Lu[24] was introduced to measure this process, which describe where the excited electron leaves as “hole” and arrives as “electron”. In Table 1, we applied the hole-electron analysis on the major electron excitation and simulated the absorption spectra with Gaussian function in Fig. 7. The distributions of hole (blue) and electron (green) of S3 were displayed with VMD software[25] and shown in Fig. 8. The S3 excitation with the biggest oscillator strength transitions from π orbitals to π* anti-bonding orbitals, which are mainly localized on 9,9’-bicarbazole.

Table 1
The absorption data of (*P*)-16[CPPL] in CH_2Cl_2.

	UV–Vis				
	E^a/eV	f^b	Hole^c	→	Electron
S1	3.71	0.18	H (32.6%), H−1(19.1%)		L(26.7%), L + 1(22.7%)
S2	3.78	0.13	H (24.5%), H−1(28.3%)		L(27.3%), L + 1(26.3%)
S3	3.99	5.11	H (21.6%), H−2(34.1%)		L(28.6%), L + 2(24.9%)
S4	4.14	1.85	H(17.6%), H−2(24.7%),H−3(23.4%)		L(20.9%),L + 2(24.9%),L + 3(17.6%)

[a] Calculated by TDDFT method. [b] Oscillator strength. [c] Orbitals involved in the major excitation (H = HOMO and L = LUMO).

UV-Vis spectrum and ECD (electronic circular dichroism) spectrum can be calculated simultaneously with Gaussian 09. The significance of rotatory strength in ECD spectrum is analogous to oscillator strengths in UV-Vis spectrum, each electron transition mode corresponds to a rotatory strength. The rotatory strength can be calculated in length representation or in velocity representation, in the former case the

strength is origin-dependent, while in the latter case the strength is origin-independent. For complete basis set situation, the results in the two representations converge to the same values. In Fig. 6(d), we simulated ECD spectrum with velocity representation since it is recommended to be used. Oscillator strength is proportional to the difference of energy level and the square of transition electric dipole moment (μ), S1 and S2 excitations have smaller energy level differences and μ (Table 2), so the oscillator strengths of S1 and S2 are far smaller than that of S3 and S4 excitations. S3 has the biggest μ and the biggest oscillator strength. The case for rotatory strength is a little more complicated, it is not only related to transition electric dipole moment (μ) and transition magnetic dipole moment (m) but also the cosine of the angle (θ) between them. The angles of S1 and S3 are bigger than 90 degree (Table 2), so the rotatory strengths are negative.

Table 2
The decomposition of transition electric dipole moment (μ).

	μ_x	μ_y	μ_z	μ/a.u.	m/a.u.	θ/deg	$g_{abs}{}^c$
S1	-0.6185	1.1814	0.4706	1.4141	7.8336	120.2	-0.3517
S2	-0.4774	0.2026	-1.0542	1.1749	15.225	30.3	0.2649
S3	7.1932	0.7530	-0.0492	7.2327	2.4319	156.3	-1.1064
S4	0.9935	-4.1464	-0.1616	4.2269	1.7521	57.9	0.7519

[a] Dissymmetry factors.

The biggest transition electric dipole moment is 7.2327 a.u. of S3 excitation. In Table 2, we found that most of the transitions are in the x direction. In order to visualize this transition, transition electric dipole moment density was integrated over the whole space to yield transition electric dipole moment. As illustrated in Fig. 9, the main transition originates from left phenylene groups to right phenylene groups along x axis.

3.4 Fluorescence and CPL (circularly polarized luminescence)

The structure on S_1 state were optimized with UDFT method. On based of optimized structure, the fluorescent emission and circularly polarized luminescence (CPL) were calculated. CPL is one of the chiroptical phenomena originating from chiral luminescence. The calculated fluorescence and CPL wavelengths are 473 nm which are displayed in Fig. 6. The fluorescence mainly arises from HOMO → LUMO excitation and the transition originates from π orbital to π* orbital of the side phenylene groups. Chiral molecules with efficient CPL are very useful for bio-sensing, bio-imaging and optoelectronic applications, and the dissymmetry factor (g_{lum}) is an important parameter for CPL. The g_{lum} can be defined as $4|m| \cdot |\mu| \cdot \cos\theta / (|m|^2 + |\mu|^2)$[26], where m and μ are the magnetic and electric transition dipole moments, respectively, θ is the angle between m and μ. In the case of m-allowed and μ-forbidden

transition, the g_{lum} will be larger. For (*P*)-16[CPPL], m and μ are 10.176 a.u. and 7.536 a.u., θ is 88.2 degree, so the g_{lum} is 0.067. It is not a surprised value since the largest g_{lum} is more than 1[27].

4. Conclusions

In summary, an interesting chiral molecule named [16]CPPL with a double half-twisted π-electron system has been explored with theoretical calculation methods. According to aromaticity analysis of the 16 phenylene groups, conjugation effect of the central group is weaker than the two sides. On the basis of frequency calculations, Raman and Raman Optical Activity (ROA) were simulated. There are obvious scattering responses near 1300nm -1400 nm and 1700 nm, which are caused by the bonds stretching in the plane of phenylene groups. UV-Vis spectrum and ECD spectrum have been calculated, S3 excitation has the biggest μ since the oscillator strength is the biggest one. The angles between μ and m of S1 and S3 are bigger than 90 degree, so the rotatory strengths are negative. The fluorescence mainly arises from HOMO → LUMO and the transition originates from π orbital to π* orbital and dissymmetry factor (g_{lum}) of CPL is 0.067.

Notes

The authors declare no competing financial interest.

Declarations

Acknowledgments

Thanks the High Performance Computation Laboratory of Changzhou University.

References

1. Brandt, J. R.; Salerno, F.; Fuchter, M. J. The Added Value of Small-Molecule Chirality in Technological Applications. Nat. Rev. Chem. 2017, *1*, 0045.
2. Ma, W.; Xu, L.; Wang, L.; Xu, C.; Kuang, H. Chirality-Based Biosensors. Adv. Funct. Mater. 2019, *29*, 1805512.
3. Glavin, D. P.; Burton, A. S.; Elsila, J. E.; Aponte, J. C.; Dworkin, J. P. The Search for Chiral Asymmetry as a Potential Biosignature in Our Solar System. Chem. Rev. 2020, *120*, 4660–4689.
4. Cintas, P. Chirality of Living Systems: A Helping Hand from Crystals and Oligopeptides. Angew. Chem. Int. Ed. 2002, *41*, 1139–1145.
5. Davankov, V. Chirality as an Inherent General Property of Matter. Chirality 2006, *18*, 459–461.
6. Peluso, P.; Chankvetadze, B. Recognition in the Domain of Molecular Chirality: From Noncovalent Interactions to Separation of Enantiomers. Chem. Rev. 2022, *122*, 13235–13400.

7. K. Senthilkumar, M. Kondratowicz, M. Lis, P. J. Chmielewski, J. Cybińska, J. L. Zafra, J. Casado, T. Vives, J. Crassous, L. Favereau, M. Stępień, Lemniscular [16]Cycloparaphenylene: A Radially Conjugated Figure-Eight Aromatic Molecule. J. Am. Chem. Soc. 2019, *141*, 7421–7427.
8. L. Palomo, L. Favereau, K. Senthilkumar, M. Stępień, J. Casado, F. J. Ramírez, Simultaneous Detection of Circularly Polarized Luminescence and Raman Optical Activity in an Organic Molecular Lemniscate. Angew. Chem. Int. Ed. 2022, *61*, e202206976.
9. T. A. Schaub, E. A. Prantl, J. Kohn, M. Bursch, C. R. Marshall, E. J. Leonhardt, T. C. Lovell, L. N. Zakharov, C. K. Brozek, S. R. Waldvogel, S. Grimme, R. Jasti. Exploration of the Solid-State Sorption Properties of Shape-Persistent Macrocyclic Nanocarbons as Bulk Materials and Small Aggregates. J. Am. Chem. Soc. 2020, *142*, 8763–8775.
10. Bauernschmitt, R.; Ahlrichs, R.; Treatment of electronic excitations within the adiabatic approximation of time dependent density functional theory, Chem. Phys. Lett. 1996, *256*, 454–464.
11. Casida, M.E.; Jamorski,C.; Casida, K.C.; Molecular excitation energies to highlying bound states from time-dependent density-functional response theory: characte-rization and correction of the time-dependent local density approximation ionization threshold, J. Chem. Phys. 1998, *108*, 4439–4449.
12. Frisch, M.J. et al., Gaussian 09, Revision D.01, Gaussian, Inc., Wallingford, CT, 2010.
13. Dreuw, A.; Head-Gordon, M.; Single-reference ab initio methods for the calculation of excited states of large molecules, Chem. Rev. 2005,*105*, 4009–4037.
14. Barone, V.; Polimeno, A. Integrated computational strategies for UV/vis spectra of large molecules in solution, Chem. Soc. Rev. 2007, *36*,1724–1731.
15. Marenich, A.V.; Cramer, C.J.; Truhlar, D.G. Universal solvation model based on solute electron density and a continuum model of the solvent defifined by the bulk dielectric constant and atomic surface tensions, J. Phys. Chem. B 2009, *113* 6378–6396.
16. J.-D. Chai, M. Head-Gordon, “Systematic optimization of long-range corrected hybrid density functionals,” J. Chem. Phys., 2008,*128*, 084106.
17. J.-D. Chai, M. Head-Gordon, “Long-range corrected hybrid density functionals with damped atom-atom dispersion corrections,” Phys. Chem. Chem. Phys., 2008,*10*, 6615–6620.
18. Schaefer, A.; Horn, H.; Ahlrichs, R. Fully optimized contracted Gaussian-basis sets for atoms Li to Kr, J. Chem. Phys. 1992,*97*, 2571–2577.
19. Schaefer, A.; Huber, C.; Ahlrichs, R.; Fully optimized contracted Gaussian-basis sets of triple zeta valence quality for atoms Li to Kr, J. Chem. Phys. 1994,*100*, 5829–5835.
20. T. Lu, F. Chen, J. Comput. Chem. 2012,*33*, 580–592.
21. Giambiagi, M., de Giambiagi, M.S., Mundim, K.C. Definition of a multicenter bond index. Struct. Chem., 1990,*1*, 423–427.
22. E. Matito, An electronic aromaticity index for large rings. Phys. Chem. Chem. Phys. 2016, *18*, 11839–11846

23. Lu,T., Manzetti, S., Wavefunction and reactivity study of benzo[a]pyrene diolepoxide and its enantiomeric forms, Struct. Chem., 2014,*25*, 1521–1533.
24. Liu, Z.; Lu,T.; Chen, Q. An sp-hybridized all-carboatomic ring, cyclo[18]carbon: Electronic structure, electronic spectrum, and optical nonlinearity. Carbon, 2020,*165*, 461–467.
25. Humphrey, W.; Dalke, A.; Schulten, K. VMD-visual molecular dynamics, J. Mol. Graph. 1996,*14*, 33–38.
26. Berova, N.; Nakanishi, K.; Woody, R.W. Circular Dichroism: Principles and Applications, 2nd ed.; Wiley-VCH:New York, NY, USA, 2000; pp. 196–197.
27. Lunkley, J.L.; Shirotani, D.; Yamanari, K.; Kaizaki, S.; Muller, G. Extraordinary circularly polarized luminescence activity exhibited by cesium tetrakis (3-heptafluoro-butylryl-(+)-camphorato) Eu(III) complexes in EtOH and $CHCl_3$ Solutions. J. Am. Chem. Soc. 2008, *130*, 13814–13815.

Figures

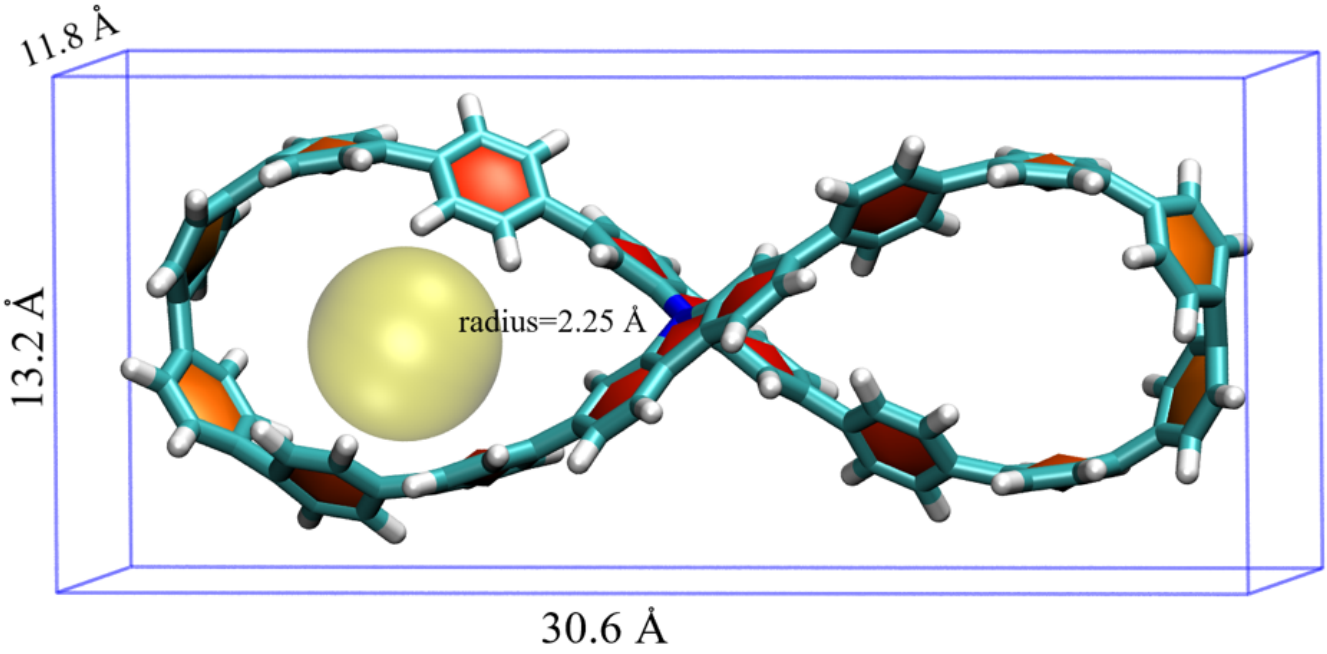

Figure 1

The structure and dimentions of (*P*)-16[CPPL].

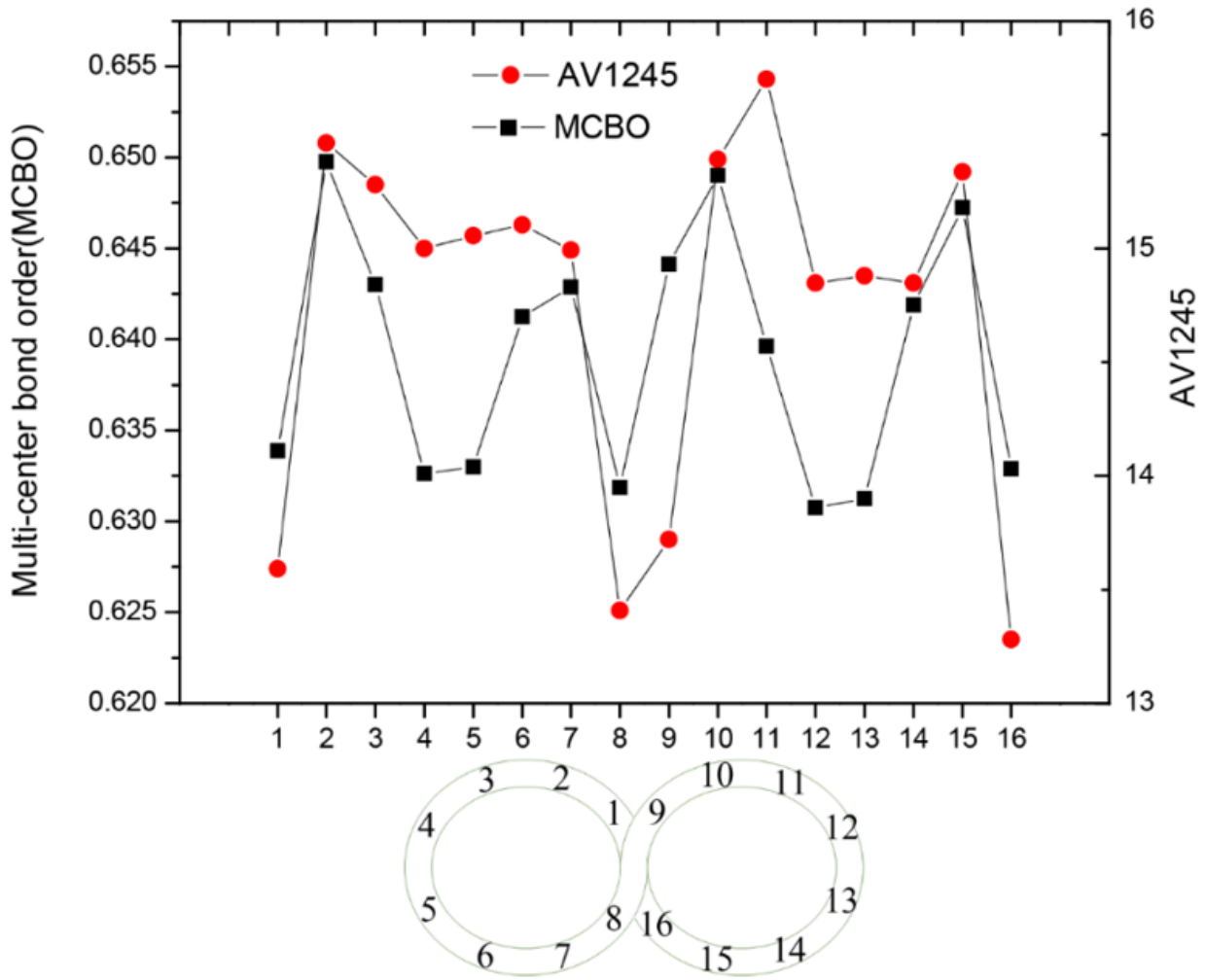

Figure 2

The aromaticity comparison of phenylene groups.

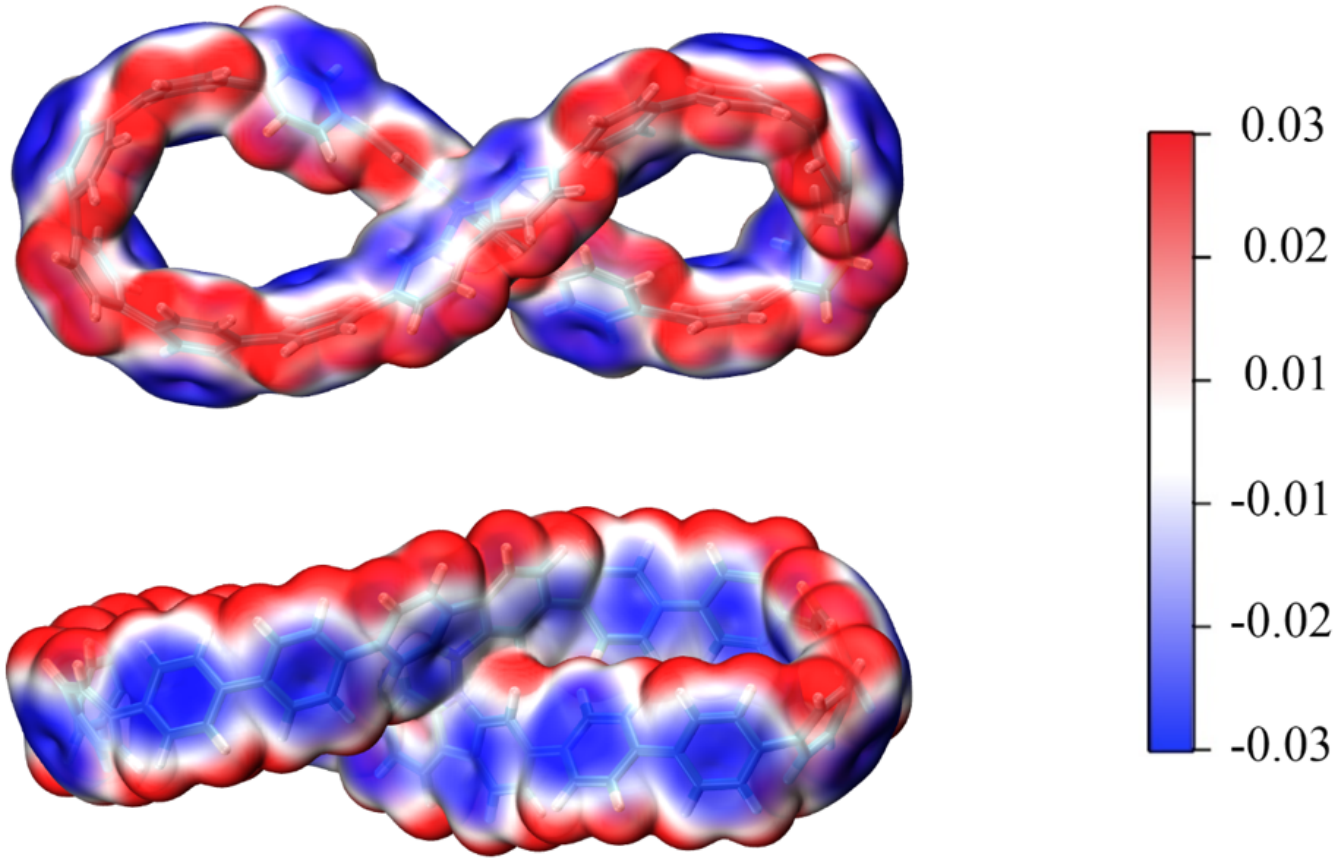

Figure 3

The isosurface maps of electrostatic potential.

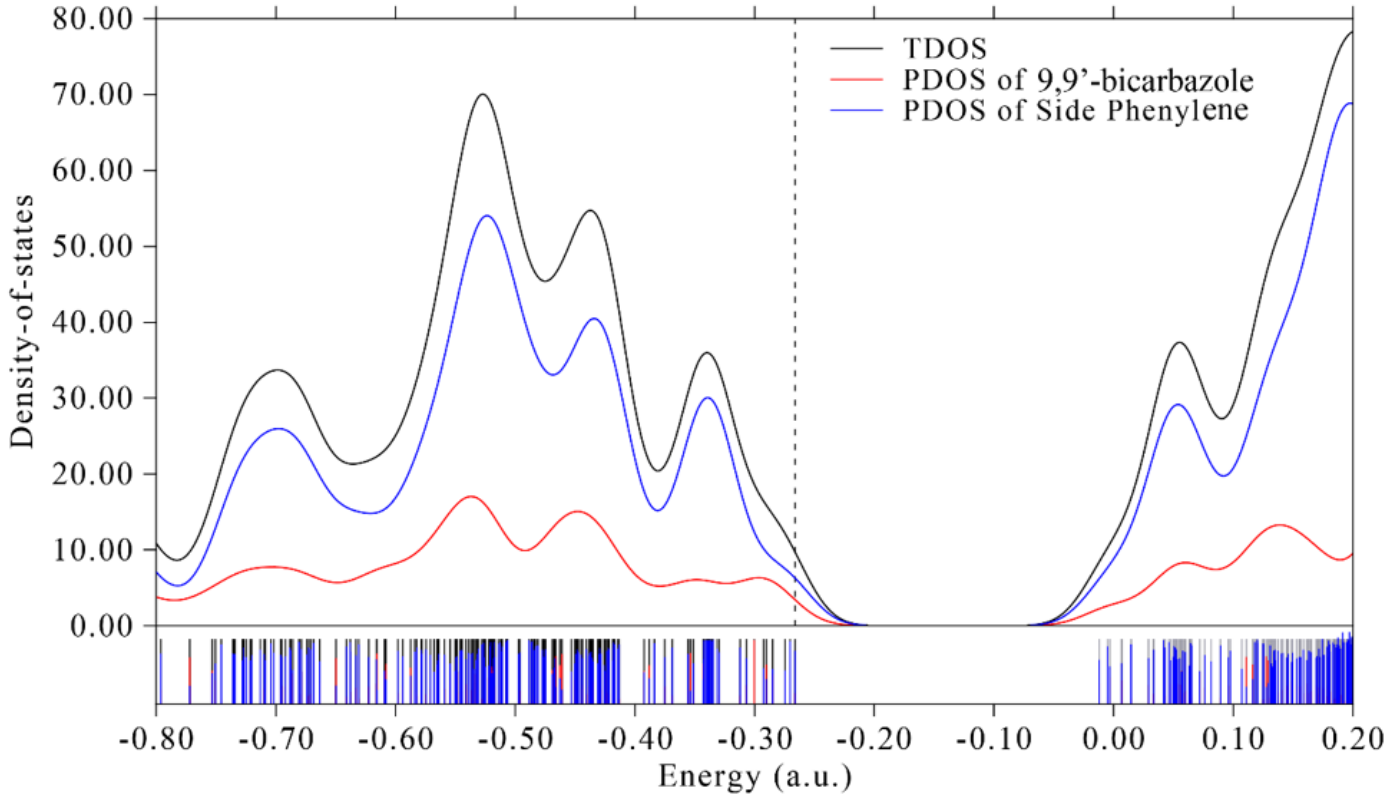

Figure 4

The density-of-states (DOS) on ground state of (*P*)-16[CPPL].

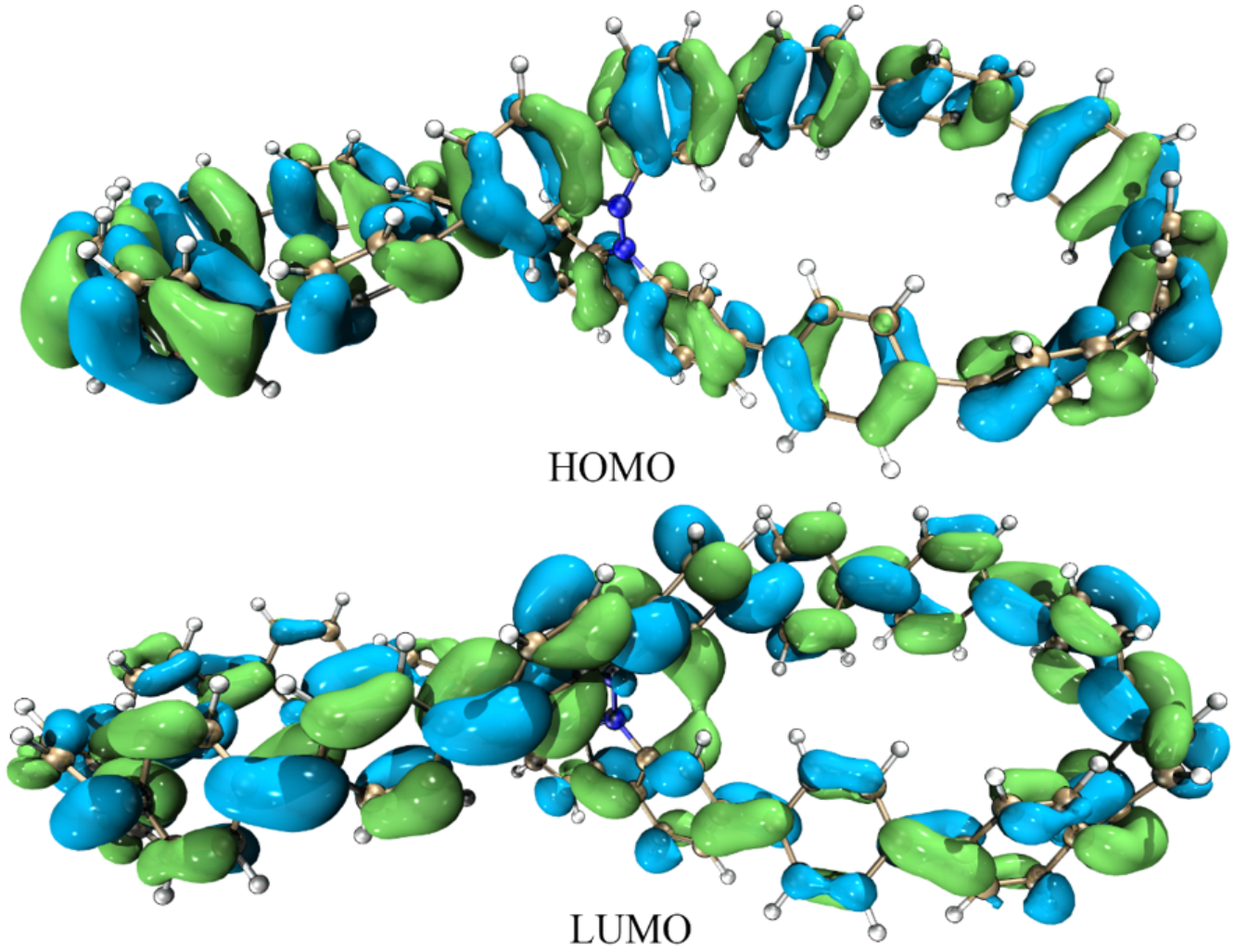

Figure 5

The highest occupied molecular orbital (HOMO) and lowest unoccupied molecular orbital (LUMO).

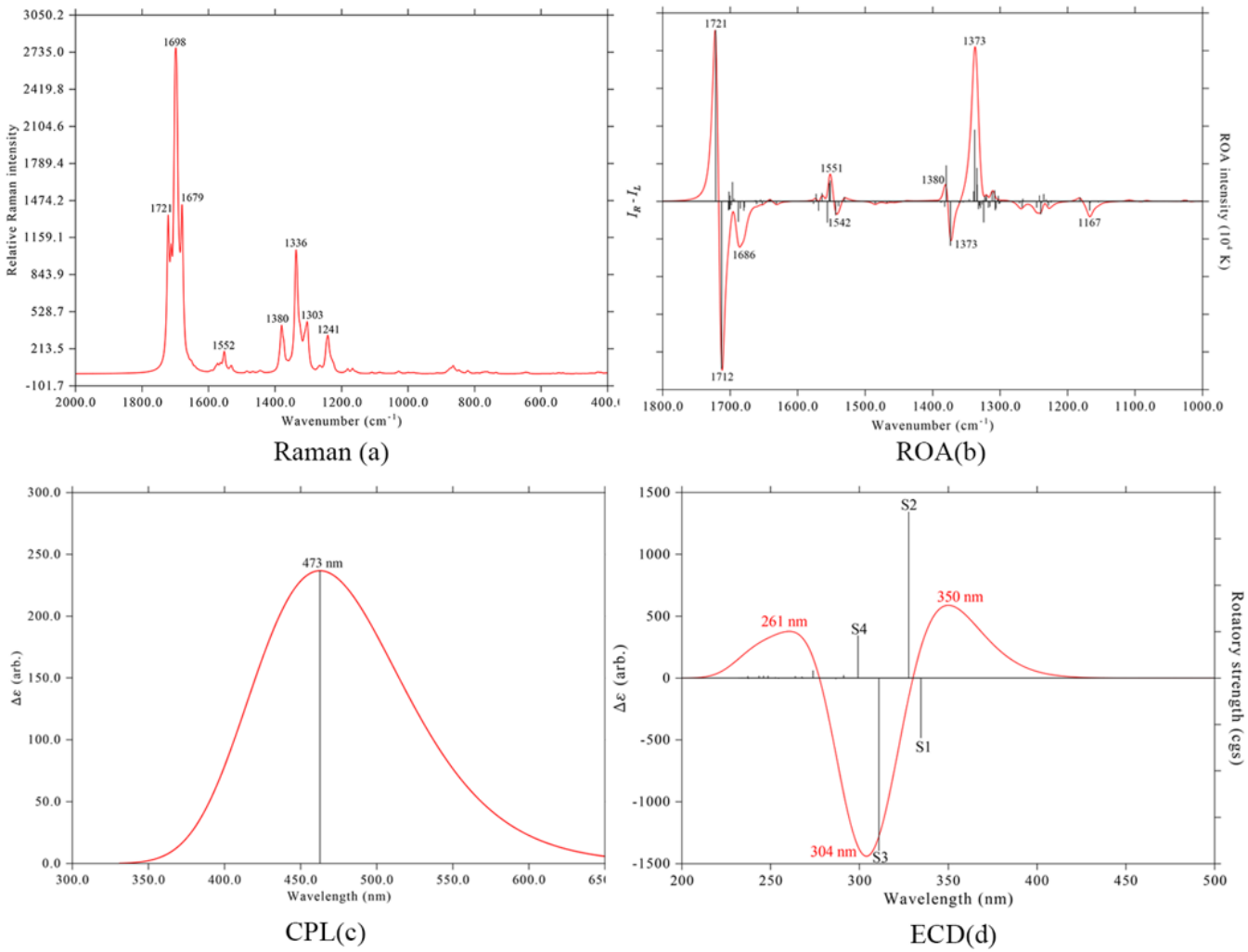

Figure 6

The Raman, ROA, CPL and ECD spectra of (*P*)-16[CPPL].

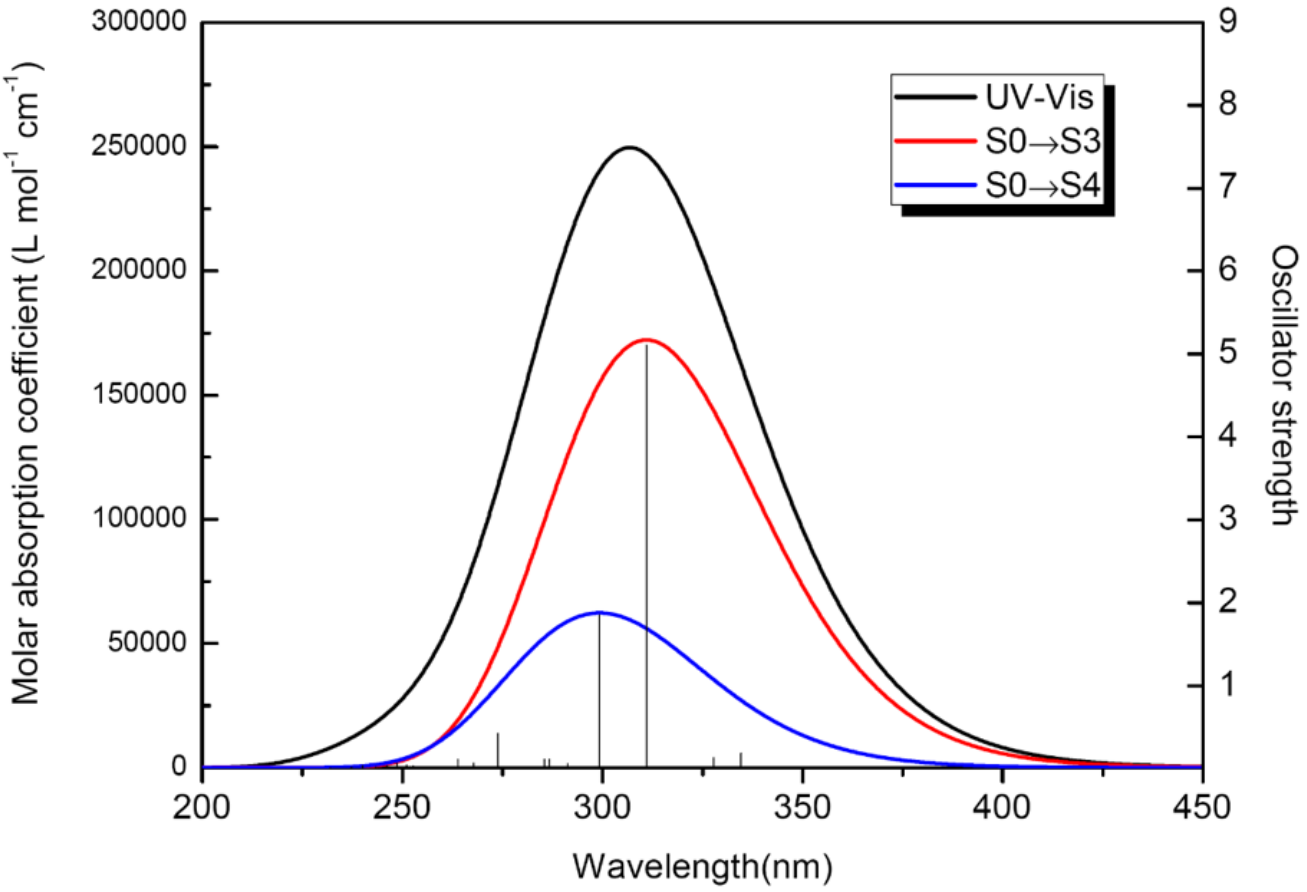

Figure 7

The simulated UV-Vis spectrum of (*P*)-16[CPPL].

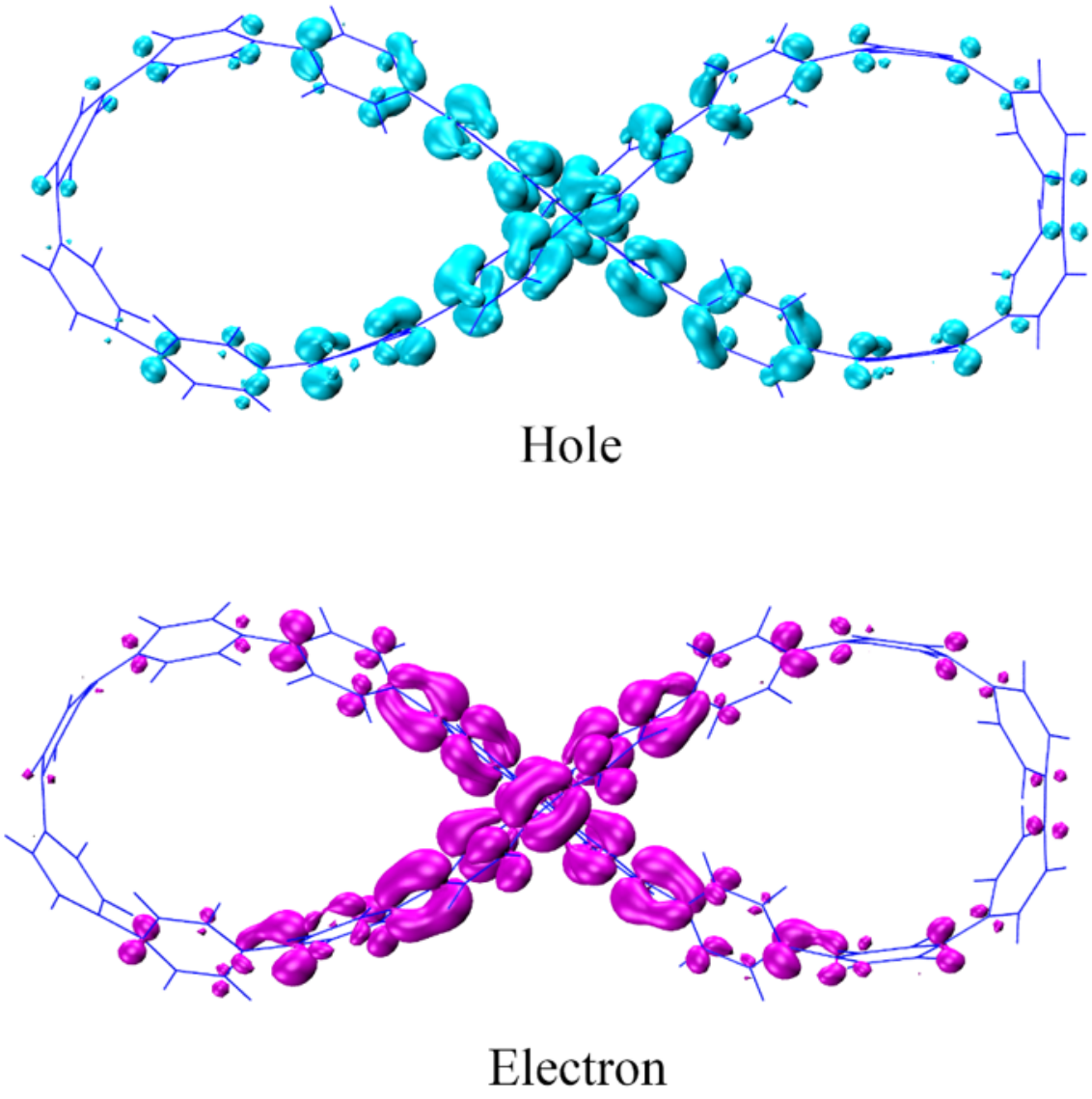

Figure 8

The hole and electron distributions of S3.

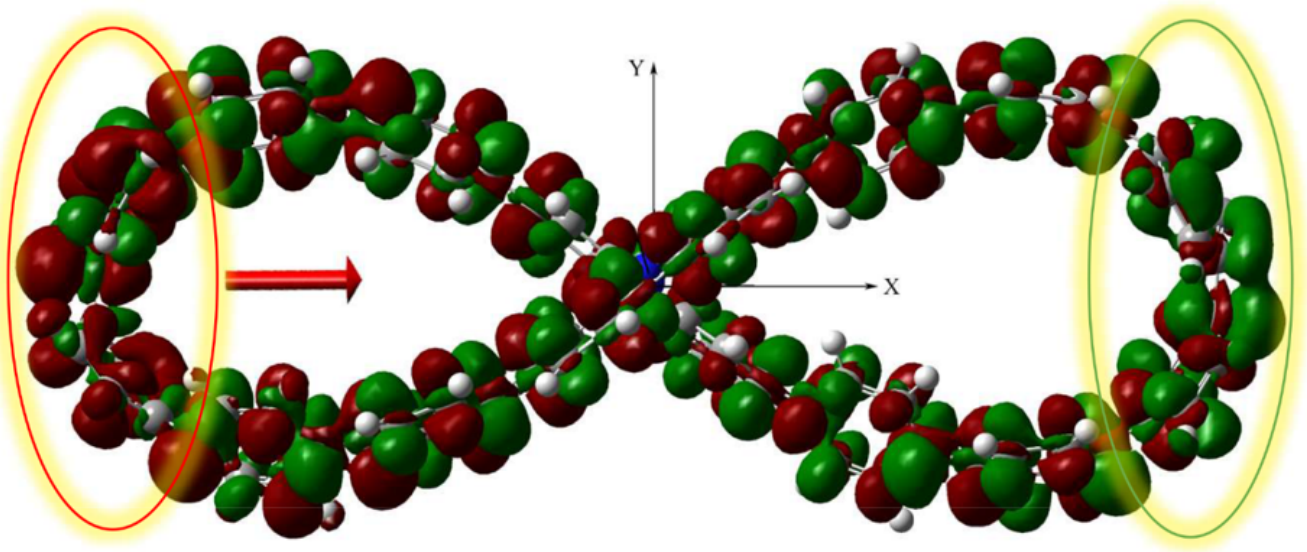

Figure 9

The transition electric dipole moment of S3.